

# HEAT TRANSFER TO FLOWING GRANULAR MEDIA

W. N. SULLIVAN\* and R. H. SABERSKY

California Institute of Technology, Pasadena, California, U.S.A.

(Received 2 August 1973 and in revised form 19 December 1973)

**Abstract**—The convective heat transfer from a flat plate immersed in a flowing granular medium has been investigated. An approximate analytical model which takes into account the particulate nature of the medium has been developed and experimental measurements were obtained. The results indicate that the Nusselt number for this configuration is influenced substantially, under certain conditions, by the non-continuous nature of the medium. A semi-empirical correlation is presented, based on experimental results obtained with four different granular materials.

## NOMENCLATURE

$c$ , specific heat of granular medium;  
 $c_p$ , specific heat of particle;  
 $d$ , particle diameter;  
 $h$ , local film coefficient;  
 $\bar{h}$ , average film coefficient;  
 $k$ , thermal conductivity;  
 $k_g$ , thermal conductivity of interstitial gas;  
 $K$ , conductance at plate surface;  
 $\bar{K}$ , particle to particle conductance;  
 $l$ , distance;  
 $L$ , length of plate;  
 $L^*$ , dimensionless length of plate;  
 $M$ , mass of particle;  
 $Nu_d$ , average Nusselt number based on  $d$ ;  
 $\bar{Nu}_L$ , average Nusselt number based on  $L$ ;  
 $\bar{Nu}_d^*$ , average Nusselt number based on  $d$  and conductivity  $k_g$ ;  
 $Pe_L$ , Péclet number based on  $L$ ;  
 $Pe^*$ , modified Péclet number, equal to  $(k/k_g)^2(d/L)^2Pe_L$ ;  
 $q$ , heat-transfer rate from particle to particle;  
 $q''$ , heat-transfer rate per unit area;  
 $t$ , time;  
 $T$ , temperature;  
 $T_w$ , wall temperature;  
 $U$ , velocity of moving granular medium;  
 $x$ , coordinate in direction of flow;  
 $y$ , coordinate normal to the flow direction.

$\gamma$ , experimental constant;  
 $\delta$ , thermal boundary-layer thickness;  
 $\Delta T$ , temperature difference;  
 $\varepsilon$ , void ratio;  
 $\eta$ , dimensionless parameter, equal to  $(L/d)^2(1/Pe_L)$ ;  
 $\theta$ , dimensionless temperature.

## 1. INTRODUCTION

THE PRESENT study concerns the convective heat transfer from surfaces immersed in a flowing granular material. The particular type of flow to be considered is that in which the adjacent material particles are in physical contact and the interstitial fluid moves passively with the particles. In such a contact-dominated flow, the motion of the interstitial fluid is not the major means of stress or heat transmission. This is in contrast with the more frequently investigated two-phase or "fluidized" systems. Contact dominated flows are found to occur in certain industrial equipment designed to heat, cool, or dry granular materials [1, 2]. It is expected that equipment of this type will be needed on a larger scale and that more exact design information will be required in order to achieve economical operation. This expectation gave the stimulus for the present investigation.

A considerable amount of research has been performed to investigate the flow characteristics of granular media (see, for example [3]). Less information is, however, available on the convective heat-transfer behavior of flowing particles. Previous work includes an experimental and theoretical study by Brinn *et al.* [4] of a contact-dominated flow in long, smooth tubes, and experimental measurements of the heat transfer from cylindrical bodies by Donskov [5] and Kurochkin [6]. Although all of the investigations consider the heat transfer from geometries having characteristic lengths

## Greek symbols

$\alpha$ , thermal diffusivity;  
 $\beta$ , dimensionless parameter, equal to  $(KL/k)(1/\sqrt{Pe_L})$ ;

\*Presently at Sandia Laboratories, Albuquerque, New Mexico.

much larger than the granular particle size, they arrive at different conclusions: Donskov as well as Kurochkin found the particle diameter to be a significant variable governing the heat transfer from cylinders, while Brinn *et al.* demonstrated that their experimental results agreed with theoretical results based on the treatment of the granular material as a one-component continuum. Another experimental study, by Harakas and Beatty [7], considered the heat transfer from a flat plate immersed in a rotating granular bed. In this work, the fine-grained materials tested were found to behave like a one-component continuum except under vacuum conditions, when substantial deviations from the continuum prediction were observed. Thus, the previously published heat-transfer data indicate that the graininess of the media can, under certain conditions, directly and substantially influence convective heat transfer. No definite parameter characterizing the importance of the granular nature of the material was specified.

The present investigation was planned to provide additional data on convective heat transfer, with emphasis on the effect of particle size. Specifically, it was decided to determine the conditions for which the particulate nature of the media affects the heat transfer and to develop suitable correlations to account for this influence.

The geometry chosen for the investigation is the thin flat plate, oriented so that the long axis of the plate is parallel to the flow field. This selection was made as it leads to one of the simplest and most basic convection problems and the results will be indicative of the general convective characteristics of granular media. In addition, the convective heat transfer from the plate for the observed flow field, a simple rectilinear flow parallel to the plate, can be solved analytically for different models of the granular medium. The experimental measurements and the analyses may then be compared with the solution for continuum flow to assess the effect of the material graininess on the heat transfer.

## 2. ANALYTICAL STUDIES

### (a) *The discrete particle model*

To study the heat transfer from a flat plate to a granular medium analytically an idealized model, called the "discrete particle model", was defined. In this model an idealized granular material is considered having the following properties:

- (i) The particles have infinite thermal conductivity, and are spherical with uniform diameter  $d$ ;
- (ii) The particles flow past the heated plate in an orderly array, as shown in Fig. 1, and extend indefinitely in the  $y$  direction. The temperature of the particles far from the heated plate is  $T_\infty$ ;

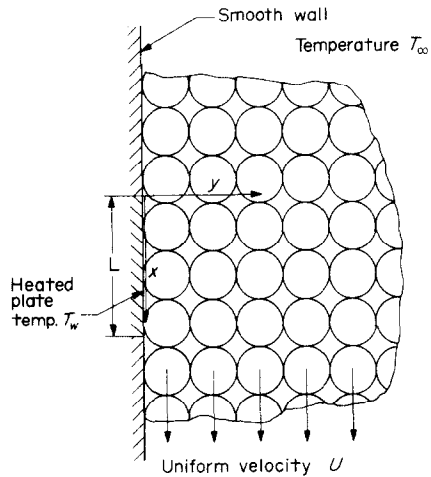


FIG. 1. Discrete particle flow past a heated plate.

- (iii) Heat is transferred only between adjacent particles, the heat flow from particle to particle given by  $q = \bar{K}\Delta T_p$ , where  $\bar{K}$  is the particle to particle conductance and  $\Delta T_p$  the temperature difference between particles. This conductance  $\bar{K}$  will generally depend on the properties of the interstitial medium and the particle diameter  $d$ ;
- (iv) Particle to particle heat transfer in the  $x$  direction is negligible compared with particle to particle heat transfer in the  $y$  direction. This simplification is analogous to the boundary-layer approximation used in continuum heat transfer.

To provide a basis for comparison with continuous media, the bulk properties of this material must be defined. Suppose that this idealized medium is exposed to a steady, one-dimensional heat flow between two parallel plates, separated by a distance  $l$  much larger than the particle diameter. The thermal conductivity  $k$  of the composite is defined by

$$k = q'' \frac{l}{\Delta T}$$

where  $q''$  is the heat flow rate per unit area, and  $\Delta T$  is the temperature difference between the parallel plates. The bulk conductivity  $k$  can be determined experimentally. This quantity  $k$  can now be related to the particle to particle conductance  $\bar{K}$  as follows. Noting that for  $n$  particles between the plates,  $l = nd$  and  $\Delta T = n\Delta T_p$ , and since there are  $1/d^2$  particles per unit area of the plate, the heat flow per particle is  $q = q''d^2$ . Using these relationships, and property (iii) of this idealized material to eliminate  $q''$ ,  $l$  and  $\Delta T$  from the definition of  $k$  yields

$$k = \frac{\bar{K}}{d}.$$

The density  $\rho$  and specific heat  $c$  of the composite are given by (neglecting the mass and heat capacity of the interstitial voids)

$$\rho = \frac{M}{d^3}, \quad c = c_p,$$

where  $M$  and  $c_p$  are the mass and specific heat of a typical particle.

The equations governing the heat transfer to the particles from the plate will now be developed. In Fig. 2 a particular row of particles moving with uniform velocity  $U$  in the  $x$  direction is examined.

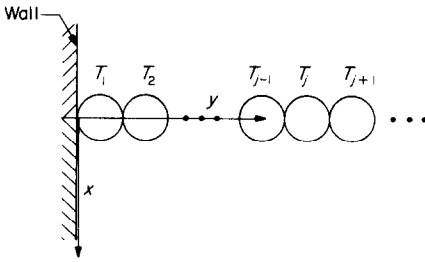


FIG. 2. Typical row of particles in a discrete particle flow.

Denoting the temperature of the  $j$ th particle in Fig. 2 by  $T_j$ , a heat balance for the  $j$ th particle at time  $t$  yields (neglecting conduction in the  $x$  direction)

$$\bar{K}[T_{j-1} + T_{j+1} - 2T_j] = Mc \frac{dT_j}{dt}, \quad j = 2, 3, \dots$$

Since the particles move at a uniform constant velocity  $U$ , the  $x$  coordinate of the particle centers,  $x = Ut$ , is used as a time scale, and the heat balance for the  $j$ th particle becomes

$$\bar{K}[T_{j-1} + T_{j+1} - 2T_j] = McU \frac{dT_j}{dx}, \quad j = 2, 3, \dots \quad (1)$$

For the case when the plate is maintained at a constant temperature  $T_w \neq T_\infty$ , the temperature of the particle adjacent to the plate must satisfy

$$\bar{K}[T_w + T_2 - 2T_1] = McU \frac{dT_1}{dx} \quad x \geq 0 \quad (2)$$

where it has been assumed that the conductance between the wall and adjacent particles is also  $\bar{K}$ .

Since heat conduction does not occur in the  $x$  direction, the temperature upstream of the plate will be  $T_\infty$  uniformly, i.e.

$$T_j = T_\infty, \quad j = 1, 2, \dots; \quad x \leq 0. \quad (3)$$

Equations (1)–(3) are conveniently expressed in terms of the dimensionless temperature  $\theta_j = (T_j - T_w)/(T_\infty - T_w)$ ,

and the dimensionless length  $x^* = x\bar{K}/McU$ . Substituting these new variables into (1)–(3) leads to

$$\theta_{j-1} + \theta_{j+1} - 2\theta_j = \frac{d\theta_j}{dx^*}, \quad j = 2, 3, \dots \quad (4)$$

$$\theta_2 - 2\theta_1 = \frac{d\theta_1}{dx^*}, \quad x^* \geq 0 \quad (5)$$

and

$$\theta_j = 1, \quad j = 1, 2, \dots; \quad x^* \leq 0. \quad (6)$$

The solution  $\theta_j(x^*)$  of this system [8] as may be verified by direct substitution into the relevant equations, is

$$\theta_j(x^*) = e^{-2x^*} \left[ I_0(2x^*) - I_j(2x^*) + 2 \sum_{m=1}^j I_m(2x^*) \right],$$

where the  $I_n$  are the modified Bessel functions of the first kind.

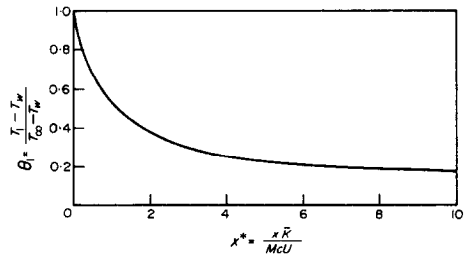


FIG. 3. Dimensionless temperature of the first particle,  $\theta_1(x^*)$ , for a constant temperature plate.

Of particular interest is  $\theta_1(x^*)$ , shown in Fig. 3, since the heat flow at the wall due to an individual particle at position  $x^*$  is given by

$$q(x^*) = \bar{K}(T_w - T_\infty)\theta_1(x^*).$$

The average heat removed per unit time by a particle traversing a plate of length  $L$  is

$$\bar{q} = \frac{1}{L} \int_0^L q(x^*) dx.$$

Since there are  $1/d^2$  particles per unit area, the average heat flux from the plate  $\bar{q}''$  is  $\bar{q}/d^2$ . Using the usual definition for the average film coefficient,  $\bar{h} = \bar{q}''/(T_w - T_\infty)$ , the Nusselt number  $\bar{Nu}_L = \bar{h}L/k$  for the discrete particle model becomes

$$\bar{Nu}_L = \frac{\bar{K}}{d^2 k} \frac{L}{L^*} F(L^*)$$

where  $L^* = L\bar{K}/McU$  and

$$F(L^*) = \int_0^{L^*} \theta_1(x^*) dx^*.$$

The Nusselt number may be expressed in terms of the bulk properties of the medium, in particular the conductivity  $k = \bar{K}/d$  and diffusivity  $\alpha = k/\rho c = \bar{K}d^2/Mc$

$$\bar{Nu}_L = \frac{d}{L} Pe_L F \left\{ \left( \frac{L}{d} \right)^2 \frac{1}{Pe_L} \right\}.$$

In this expression  $Pe_L$  is the Péclet number, defined as  $Pe_L = UL/\alpha$ . This result is shown in Fig. 4, along with

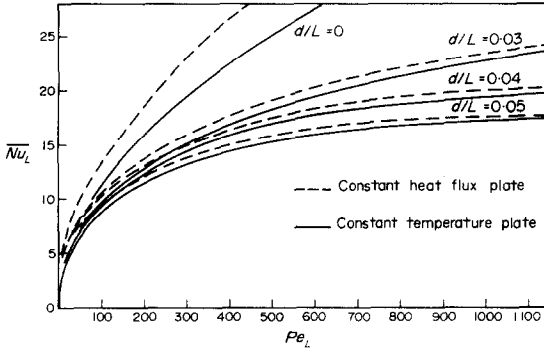


FIG. 4. Average Nusselt number as a function of Péclet number for the discrete particle model.

an analogous solution [8] for the constant heat flux plate. While Fig. 4 is illustrative in that it shows the influence of  $d/L$  on the  $\bar{Nu}_L$  vs  $Pe_L$  curves it should be pointed out that these curves could be replaced by a single one by using the coordinates

$$\bar{Nu}_d \quad \text{and} \quad \left( \frac{L}{d} \right)^2 \frac{1}{Pe_L}.$$

(b) Comparison of the discrete particle model with a one-component continuum

For purposes of comparison, the heat transfer from the flat plate associated with the uniform flow of a one-component continuum with properties  $k$  and  $\alpha$  can be determined within the boundary-layer approximation of negligible conduction in the  $x$  direction. For this continuum flow, the energy equation is

$$\frac{\partial^2 T}{\partial y^2} = \frac{U}{\alpha} \frac{\partial T}{\partial x} \tag{7}$$

and with the constant temperature flat plate, the boundary conditions are

$$\left. \begin{aligned} T(0, x) &= T_\omega, & x &\geq 0 \\ T(0, x) &= T_\infty, & x < 0 \\ T(\infty, x) &= T_\infty. \end{aligned} \right\} \tag{8}$$

Noting that (7) is identical in form to the well-known heat-diffusion equation, the solution for the local film coefficient is given by

$$h(x) = \frac{q''(x)}{T_\omega - T_\infty} = \frac{k}{(\sqrt{\pi})} \frac{1}{\sqrt{(\alpha x/U)}}.$$

Integrating this expression over a plate of length  $L$  yields the average Nusselt number

$$\bar{Nu}_L = \frac{2}{(\sqrt{\pi})} \sqrt{(Pe_L)}. \tag{9}$$

To compare the heat-transfer result of the discrete particle model to the continuum, the ratio of the Nusselt numbers obtained for these different materials is illustrative.

$$R = \frac{\bar{Nu}_L \text{ (discrete particles)}}{\bar{Nu}_L \text{ (continuum)}} = \frac{(\sqrt{\pi}) F(\eta)}{2 (\sqrt{\eta})}$$

where

$$\eta = \left( \frac{L}{d} \right)^2 \frac{1}{Pe_L}.$$

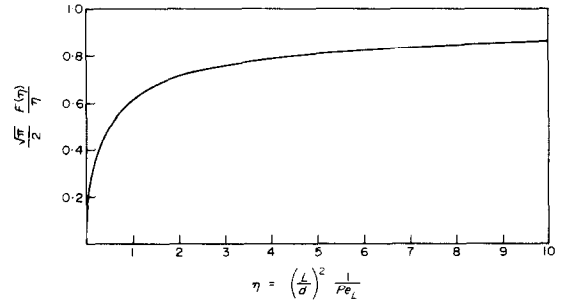


FIG. 5. Comparison of heat transfer for the discrete particles and a one-component continuum.

This ratio is plotted in Fig. 5, and the curve indicates that for  $\eta < 10$ , the discrete particle model deviates considerably from the continuum prediction. Of interest is the fact that this deviation is a function of the single dimensionless group  $\eta$ . This variable can be given a physical interpretation by means of the continuum solution, which shows that the dimensionless thermal boundary layer thickness  $\delta/L$  is proportional to  $1/\sqrt{(Pe_L)}$ . Thus,

$$\frac{\delta}{d} \propto \frac{L}{d} \frac{1}{(\sqrt{Pe_L})} = (\sqrt{\eta})$$

represents the ratio of the thermal boundary-layer thickness to the particle diameter. It is quite plausible, therefore, that for larger values of  $\eta$  the continuum solution is a good approximation to the solution obtained from the discrete particle model. The two solutions differ, however, for lower values of  $\eta$ , that is when the thermal boundary layer is of the order of the particle size or smaller.

(c) *Single resistance model*

One further comparison is of interest, that between the heat flux calculated from the discrete particle model (which has thermal resistances between each particle) and a continuum which, however, has a single thermal resistance at the wall. Such a comparison should indicate to what extent the overall heat transfer from the wall is influenced by the granular structure which is not adjacent to the wall.

The temperature field associated with a continuum that has a thermal conductance  $K$  at the plate surface must satisfy the convective heat-transfer equation (7), with the first boundary condition in (8) replaced by

$$-k \frac{\partial T}{\partial y}(0, x) = K[T_w - T(0, x)], \quad x \geq 0$$

where  $T_w$  is the constant temperature of the plate. The quantity  $K$  is the conductance per unit area of the plate, related to the particle to particle conductance through  $K = \bar{K}/d^2 = k/d$ . The solution to (7) with this boundary condition is found in [9] and yields the local film coefficient

$$\frac{h(x)}{k} = \frac{K}{k} e^{\beta^2} \operatorname{erfc}[\beta_x].$$

In this expression,  $\beta_x = Kx/k \sqrt{(1/Pe_x)}$  and  $\operatorname{erfc}[\beta_x]$  is the complimentary error function. Averaging this local film coefficient over the plate gives

$$\begin{aligned} \bar{Nu}_L &= \frac{\bar{h}L}{K} = \frac{KL}{k} \left\{ \frac{1}{\beta^2} \left( e^{\beta^2} \operatorname{erfc}(\beta) - 1 + \frac{2}{\sqrt{\pi}} \beta \right) \right\} \\ &= \frac{KL}{k} f(\beta) \end{aligned}$$

where

$$\beta = \frac{KL}{k} \sqrt{(1/Pe_L)}.$$

To compare this result with the discrete particle solution, the latter must be expressed in terms of the same variables. For the discrete particle model with a constant temperature plate, the Nusselt number was seen to be

$$\bar{Nu}_L = \frac{d}{L} Pe_L F(\eta)$$

with  $\eta$  defined as

$$\eta = \left( \frac{L}{d} \right)^2 \frac{1}{Pe_L}.$$

But,

$$\frac{L}{d} = \frac{KL}{Kd} = \frac{KL}{k},$$

hence  $\eta = \beta^2$ . Thus,

$$\bar{Nu}_L = \frac{KL}{k} \frac{F(\beta^2)}{\beta^2} = \frac{KL}{k} F^*(\beta)$$

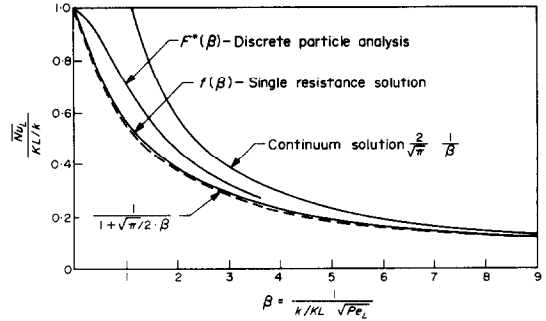


FIG. 6. Comparison of the discrete particle solution with a continuum with conductance  $K$  at the plate surface, for a constant temperature plate.

for the discrete particles. In Fig. 6 the function  $F^*(\beta)$  associated with the discrete particle analysis is shown, as is the function  $f(\beta)$  for the continuum with a single resistance at the wall. Also shown is the numerically approximate form for  $f(\beta)$

$$f(\beta) = \frac{1}{1 + \beta(\sqrt{\pi})/2} \quad (10)$$

which corresponds to

$$\bar{Nu}_L = \frac{1}{\frac{k}{KL} + \frac{(\sqrt{\pi})}{2} \frac{1}{\sqrt{(Pe_L)}}} \quad (11)$$

For large  $\beta$ , both  $f(\beta)$  and  $F^*(\beta)$  converge to the asymptote  $2/(\beta\sqrt{\pi})$ , this asymptote corresponding to the continuum solution,

$$\bar{Nu}_L = \frac{2}{(\sqrt{\pi})} \sqrt{(Pe_L)}.$$

For smaller  $\beta$ , the continuum with resistance at the wall also behaves like the discrete particle model. It would seem, therefore, that a reasonable approximation for the Nusselt number in a discrete particle flow would be obtainable by considering the medium as continuous except for a special thermal resistance at the wall. Indeed, a more detailed analysis applied to the constant heat flux plate [8] indicates that the single resistance approximation improves, as one would expect, if the wall to particle resistance is greater than the particle to particle resistance.

## 3. EXPERIMENTAL APPARATUS

The flow apparatus, shown schematically in Fig. 7, consists of three basic parts, from top to bottom: the supply hopper, the plexiglass test section, and the regulating valve.

The regulating valve is basically an adjustable clamp acting on a rubber membrane. This clamp provides a continuous adjustment of the mass flow rate through

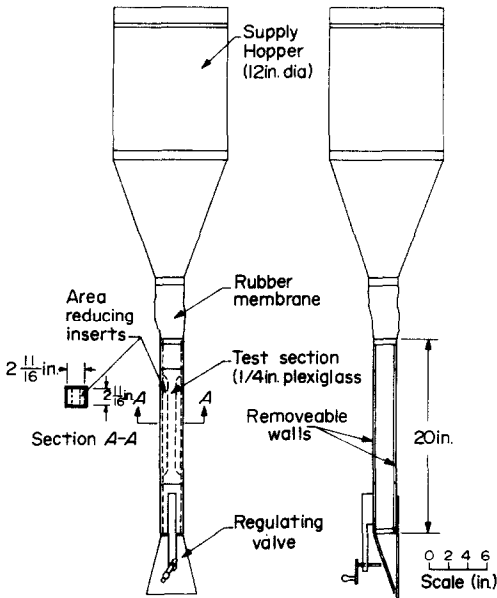


FIG. 7. Schematic diagram of the flow apparatus.

the valve and is the means by which the velocity in the channel is controlled.

The test section is constructed of plexiglass to facilitate visual observation of the flow. Removable front and rear sections are provided for the mounting of models in the flow field. The flow area of the test section can be changed by adding area-reducing inserts, shown by the dotted lines in Fig. 7. These inserts permit higher velocities to be maintained in the test section while keeping the mass flow rate within reasonable limits.

The supply hopper has considerably larger volume than the test section and enables flow to persist in the channel for several minutes. In the heat-transfer experiments, continuous flow is required for an extended period, necessitating periodic refilling of the supply hopper through its open top.

The system as described is capable of maintaining a continuous velocity in the channel between approximately 0.5 and 5.0 cm/s, the exact limits depending on the particular material used in the flow. The lower limit on the velocity results from the inability of the flow valve to pass a steady flow without clogging and the upper limit from the difficulty in maintaining the level in the supply hopper. The obtainable range, however, was entirely sufficient for the present program.

The flat plate used for the heat-transfer experiment is shown in Fig. 8. A pair of heated copper plates are imbedded on opposite sides of the thin plexiglass holder which is placed in the flow channel with its long axis coincident with the channel centerline. The resulting symmetric flow will expose each plate to a

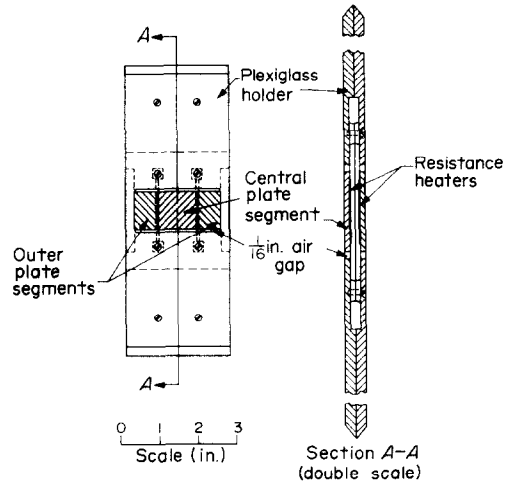


FIG. 8. Schematic diagram of the flat plate model.

similar flow field. Referring to the front view of the plate (Fig. 8), each plate is split into three segments separated by thin air gaps. The actual heat-transfer measurements are made only on the central segment of the plate. The outer segments act as guards to ensure all the heat supplied to the central heater is actually transmitted to the flow. The isolation of the central plate from the edges also ensures the two-dimensionality of the heat transfer. All the plate segments are provided with chromel-alumel thermocouples to permit the balancing of the system and the measurement of heat-transfer coefficients.

A plate length (2.54 cm) was selected, using the discrete particle analysis as a guide, so that measurable non-continuum effects would be encountered for the materials under investigation. A provision is made, however, to replace the 2.54-cm long plate by a similar one of 1.52 cm in length in the same holder, for the purpose of permitting the independent variation of the plate length to particle diameter ratio.

Heat losses from the central plates are a source of error which must be carefully controlled, in view of the low heat-transfer coefficients encountered with the typically poor-conducting granular materials under investigation. The major losses are due to heat conduction from the central segment to the plate holder, and to those outer segments which are not at exactly the same temperature as the central segment. Estimates of these losses [8] indicate that for typical operating conditions these losses constitute less than 6 per cent of the heat supplied to the central segment.

The distance from the surface of the plates to the walls of the flow channel, both with and without the area-reducing inserts installed, is many times the thermal boundary-layer thickness estimated using a continuum theory. The channel wall is therefore

expected to be effectively an infinite distance from the plate surface. This contention is checked experimentally by comparing heat-transfer data obtained using the channel with and without the area-reducing inserts installed.

#### 4. THE GRANULAR MEDIA

Four granular materials were selected for the experimental investigation. Three of these materials consist of hard, spherical particles with a narrow distribution of diameters about the mean. A fourth material, a common fine-grained sand, has irregularly shaped particles of relatively nonuniform size.

In order to interpret the experimental results the thermal conductivity, thermal diffusivity, mean particle

interstitial medium and  $k$  is the bulk conductivity of the heterogeneous granular substance. In arriving at this ratio it was assumed that the heat transfer from particle to particle is by conduction through the interstitial gas. The heat conduction through areas of direct contact and the radiative exchange was taken to be negligible. This assumption is valid for the test conditions of the present experiments in which the pressure was atmospheric and the temperature differences were small.

In the results to be presented the independent parameters cover the following ranges:  $0.05 < k_g/k < 0.14$ ;  $12 < L/d < 120$ ; and  $100 < Pe_L < 9000$ . The void ratio  $\epsilon$  is essentially constant for the three materials with

Table 1

	Glass traffic beads	Glass impact beads	Mustard seed	Fine-grained sand
Mean particle size (in)	0.013	0.053	0.085	0.008
Standard deviation (%)	2.4	1.0	1.2	2.5
Bulk density (specific weight)				
Critical state	1.5	1.7	0.7	1.5
Dense state	1.6	1.8	0.8	1.7
Void ratio (%)				
Critical state	73	71	74	91
Dense state	60	59	59	63
Thermal diffusivity $\times 10^6$ (ft <sup>2</sup> /s)				
Critical state	1.7	1.7	0.9	3.1
Dense state	2.1	1.8	0.9	3.3
Thermal conductivity (Btu/h-ft <sup>2</sup> -°F)				
Critical state	0.12	0.11	0.08	0.2
Dense state	0.16	0.13	0.09	0.3

diameter, and the flowing density of the materials must be determined. Thermal properties were determined by transient methods outlined in [4, 8]. All the thermal properties were measured in the flowing (critical) and densely packed states, although only the former were used for reduction of experimental data. Particle size and size distribution were measured optically, using average values from a large number of measurements. The results of the property measurements are summarized in Table 1.

#### 5. EXPERIMENTAL RESULTS

The experimental results will be presented in terms of the average Nusselt number ( $\overline{Nu}_L = \overline{h}L/k$ ) and the Péclet number  $Pe_L = UL/\alpha$ . In addition a brief dimensional analysis shows that three further parameters should be considered. Two of these are geometrical ratios; the plate length to the characteristic particle dimension,  $L/d$ , and the void ratio  $\epsilon$ . The third parameter is  $k_g/k$  where  $k_g$  is the conductivity of the

spherical particles, which all had a narrow size distribution. The void ratio for the sand with its irregularly shaped particles was different.

In Fig. 9,  $\overline{Nu}_L$  vs  $Pe_L$  data are shown for the two types of glass beads and the fine-grained sand for flow over the 1.52-cm long plate. On this same plot is given the expected result for the flow of a continuous material, and the experimental data differ significantly from the continuum prediction. These differences, which are relatively small at low Péclet numbers, grow considerably at higher Péclet numbers. This divergence, qualitatively similar to the divergence observed with the discrete particle model, indicates clearly that the heat transfer is influenced by the noncontinuous nature of the granular medium.

An attempt has been made to fit the data points in Fig. 9, with curves of the form

$$\overline{Nu}_L = \frac{1}{\gamma + \frac{(\sqrt{\pi})}{2} \sqrt{(1/Pe_L)}} \quad (12)$$

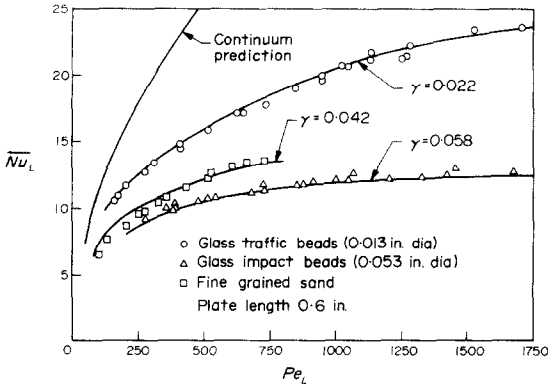


FIG. 9. Nusselt number vs Péclet number data for the 0.6 in. plate.

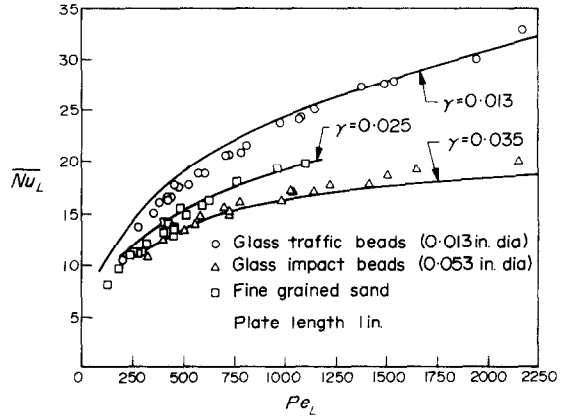


FIG. 10. Nusselt number vs Péclet number data for the 1 in. plate.

where  $\gamma$  is a constant. This constant is selected to provide the best fit to the experimental data and each solid line in Fig. 9 corresponds to a different value of  $\gamma$ . For the range of the experimental data considered, this function adequately describes the Péclet number dependence of the Nusselt number, and thus one may conclude that in general  $\gamma$  should be some function of the remaining dimensionless variables namely  $k_g/k$ ,  $L/d$  and  $\epsilon$ . The determination of this function may be simplified by noting that the function (12) is identical in form to the numerically approximate formula (11) discussed earlier to describe the heat transfer from a constant temperature plate with a thermal conductance  $K$  at the plate surface, i.e.

$$\overline{Nu}_L = \frac{1}{\frac{k}{KL} + \frac{(\sqrt{\pi})}{2} \sqrt{1/Pe_L}}$$

This correspondence suggests that  $\gamma$  might be given a physical interpretation, that is,  $\gamma = k/KL$ , where in the actual flow of particles the "effective"  $K$  is due to the presence of the relatively poor-conducting interstitial air in the irregularly shaped region between the plate surface and the first row of particles. If such an interpretation is correct, this conductance  $K$  should not depend on the heated length  $L$  of the plate. Thus, if a particular material used with a plate of length  $L$  has associated with the heat-transfer data a certain  $\gamma$ , then this material when flowing over a plate of length  $L'$  should yield heat-transfer data represented by the same function (12) with  $\gamma$  replaced by  $\gamma' = \gamma L/L'$ . In Fig. 10 are shown data for the same materials as in Fig. 9, but for heated plates 2.54-cm long. The  $\gamma$ 's associated with the solid lines of Fig. 10 are derived from the  $\gamma$ 's of Fig. 9 by multiplying by the length ratio 0.6. The agreement of the solid curves in Fig. 10 with the data is good, supporting the proposed physical interpretation of  $\gamma$ . Figure 11 shows two curves corresponding

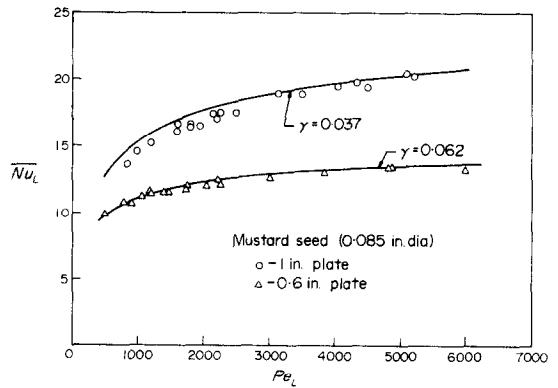


FIG. 11. Nusselt number vs Péclet number data for the mustard seed, using the 0.6 and 1 in. plate.

to the different length plates for mustard seed, this low diffusivity material covering a relatively high range of Péclet numbers. For these data the  $\gamma$ 's associated with the different length plates are again in the ratio 0.6, the length ratio.

The above results indicate that the concept of an effective thermal conductance at the plate is a useful one. In the discrete particle analysis, it was assumed that the conductance at the wall would be the same as that existing between adjacent rows of particles. This assumption, together with the assumptions of a regular geometry and of infinitely conducting particles, permitted the determination of the conductance  $K$  in terms of the bulk conductivity,  $K = k/d$ . An actual particle flow differs from this both in the geometry of the packing and particle conductivity. It may be fruitful, therefore, to consider in more detail the factors affecting the wall conductance. With the notion that the conductance is due to the thermal interaction between the wall and the first row of particles, it follows that for a particular set of particles, the conductance should be



proportional to the conductivity of the interstitial gas  $k_g$ , provided that heat conduction through the physical contacts and thermal radiation across the voids are a negligible portion of the total heat transferred. Furthermore, with the same assumptions, the conductance  $K$  should be inversely proportional to the average thickness of the gas film between the heated plate and the particles. Noting that this average thickness, for geometrically similar particles at the same void ratio, is proportional to the particle characteristic length  $d$ , it is postulated that

$$K = \frac{1}{\chi} \frac{k_g}{d} \quad (13)$$

where  $\chi$  is a dimensionless proportionality constant which is independent of the thermal properties of the interstitial gas or the particles. This  $\chi$  may be interpreted as the ratio of the thickness  $l$  of a uniform gas film, with a conductance  $K = k_g/l$ , to the particle characteristic length  $d$ . For geometrically similar arrangements of particles at the plate surface,  $\chi$  should have the same numerical value. However, any changes in physical conditions which might affect the local geometrical arrangement of particles near the wall will generally change  $\chi$ . For example, the presence of a rough plate as opposed to a smooth one, or the use of irregularly shaped particles instead of spherical particles will affect the local particle geometry and therefore  $\chi$ .

The validity of (13) must, of course, be verified by experimental data. To examine the verifiable consequences of (13), substitution of this relationship into (12) yields

$$\frac{\bar{h}d}{k_g} = \overline{Nu}_d^* = \frac{1}{\chi + \frac{(\sqrt{\pi})}{2} \sqrt{(1/Pe_L^*)}} \quad (14)$$

where  $\overline{Nu}_d^*$  is now the Nusselt number based on the particle diameter  $d$  and gas conductivity  $k_g$  and a modified Péclet number has been defined as

$$Pe_L^* = \left(\frac{k}{k_g}\right)^2 \left(\frac{d}{L}\right)^2 Pe_L.$$

This parameter is closely related to  $\eta$  which was introduced earlier. It then follows from (13) that the heat-transfer data for geometrically similar particle arrangements such as occurs with spherical particles flowing over a smooth plate, should lie on a single curve with the Nusselt number  $\overline{Nu}_d^*$  and Péclet number  $\overline{Pe}_L^*$  as coordinates. In Fig. 12, all the results for spherical particles are shown in terms of this modified coordinate system, and the data do in fact lie reasonably close to a single curve. Furthermore, this single curve is well represented by the function (14) with  $\chi = 0.085$ , i.e. for an "effective" air film thickness about 1/10 of a

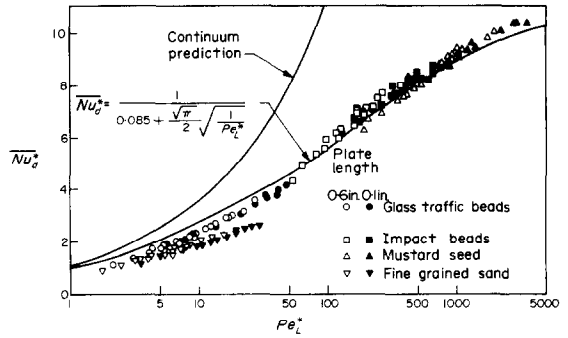


FIG. 12. Nusselt  $\overline{Nu}_d^*$  number vs modified Péclet number data for all materials tested, with both plate lengths.

particle diameter. The data for the fine-grained sand, with its irregularly shaped particles, lies distinctly below the spherical particle data. This difference is consistent with the physical interpretation of the wall conductance discussed above; the sand, with its irregularly shaped particles and different void ratio should not necessarily have the same value of  $\chi$ . In addition it has to be remembered that the reasoning leading to equation (14) has been based on the assumption that the dominant heat-transfer mechanism is pure conduction through the interstitial gas. The actual conditions in this respect must also be expected to cause some deviation of the data from a single curve.

#### DISCUSSION AND CONCLUDING REMARKS

The experimental data presented shows that the treatment of granular media consisting of spherical particles as effectively a continuum with a thermal conductance  $K$  at the wall leads to a reasonable description for the heat transfer from the flat plate immersed in a granular flow. Equation (14), containing one empirical constant, correlates the experimental results reasonably well. For the present experiments a constant of  $\chi = 0.085$  provided the best representation. Substantial errors can occur if one attempts to predict heat-transfer rates for granular media on the basis of a continuous substance with perfect conductance at the wall. The extent of the deviation will be a function of a single dimensionless group, the modified Péclet number,  $Pe_L^*$ .

The results of the present study also show that the nature of the heat transfer from the flat plate differs considerably, depending on the magnitude of Péclet numbers encountered. For low modified Péclet numbers,  $Pe^* < 2$ , the granular materials function as a single component continuum and the heat transfer from the flat plate is governed solely by the bulk thermal properties  $k$  and  $\alpha$ . Those properties characterizing the detailed structure of the granular material, that is, the particle diameter and gas conductivity,

have no direct influence on the heat transfer for these low modified Péclet numbers. For large values of the modified Péclet number (greater than 1000), the heat transfer is dominated by the thermal resistance at the wall; as a result the film coefficient is close to being inversely proportional to the particle diameter and directly proportional to the interstitial gas conductivity. In between these two extremes of modified Péclet numbers is a large transitional regime where both the bulk and structural properties of the medium influence the heat transfer. The notion of two different heat-transfer regimes corresponding to the continuous or noncontinuous behavior of granular materials can be used to explain the differences in the conclusions of Brinn *et al.* [4] as compared to those by Kurochkin [6] and Donskov [5]. In Brinn's experiments with fine-grained materials flowing through tubes, the maximum modified Péclet number encountered (based on the tube length and average particle diameter), is approximately 4, and thus any non-continuum effects would be small and difficult to detect through the experimental scatter. The experiments by Donskov extended to modified Péclet numbers as high as 3000 and he noted a very definite effect of the grain size on heat transfer. Kurochkin also reported such an effect and although [6] does not contain enough information to compute Péclet numbers, it may be inferred that they were relatively high. Most of the data in the study of Harakas and Beatty [7] correspond to low modified Péclet numbers and the continuum behavior observed by these investigators is consistent with the results given here. There are, however, in [7] some results taken at modified Péclet numbers in the range 10–50 which differ somewhat from the proposed correlation. This disagreement is believed to be partially due to possible differences in the thermal property measurements, and partially due to differences in flow pattern.

In the experiments by Beatty and Harakas a flat plate was mounted on a rotating arm and moved through a bed of particles. The packing density under these circumstances, could well be different from that for the present experiments and could even vary between the inside and the outside surface. These factors could contribute to the experimental differences.

*Acknowledgements*—The research presented in this paper was sponsored by grants from the National Science Foundation (Grant GK-30524) and the Procter & Gamble Company. This important financial support is greatly appreciated. It is also a pleasure to acknowledge the technical advice and recommendations we received from Mr. Robert C. Kramer of the Procter & Gamble Company, and to thank him for his interest in this project.

#### REFERENCES

1. V. W. Uhl and W. L. Root, Heat transfer to granular solids in agitated units, *Chem. Engng Progr.* **63**(7), 81–92 (July 1967).
2. R. L. Kramer, Director of Engineering Development, The Procter & Gamble Co., Private Communication.
3. A. W. Jenike, P. J. Elsey and R. H. Woolley, Flow properties of bulk solids, *Proc. Am. Soc. Test. Mater.* **60**, 1168–1181 (1960).
4. M. S. Brinn *et al.*, Heat transfer to granular materials, *Ind. Engng Chem.* **40**(4), 1050–1061 (June 1948).
5. S. V. Donskov, Heat loss from a round cylinder in transverse flow of a granular medium, *Teploenergetika* **5**(10) (October 1958).
6. Yu. P. Kurochkin, Heat transfer between tubes of different sections and a stream of granular material, *J. Engng Phys.* **10**(6), 447–449 (1966).
7. N. K. Harakas and K. O. Beatty, Moving bed heat transfer: effect of interstitial gas with fine particles, *Chem. Engng Progr. Symp. Ser.* **59**(41), 122–128 (1963).
8. W. N. Sullivan, Heat transfer to flowing granular media, Ph.D. Thesis, California Institute of Technology (September 1972).
9. H. S. Carslaw and J. C. Jaeger, *Conduction of Heat in Solids*, 2nd Edn, p. 74. Oxford University Press, Oxford (1959).

#### TRANSFERT DE CHALEUR A UN MILIEU GRANULAIRE EN ECOULEMENT

**Résumé**—On étudie la convection thermique à partir d'une plaque immergée dans un milieu granulaire en écoulement. Un modèle analytique approché tient compte de la nature divisée du milieu et on a fait des expériences. Les résultats indiquent que le nombre de Nusselt est fortement influencé, sous certaines conditions, par la nature discontinue du milieu. On présente une relation semi-empirique basée sur des résultats expérimentaux obtenus avec quatre matériaux granulaires différents.

#### EINSPRITZKÜHLUNG BEI TURBULENTEM FREISTRRAHL UND AUSGEPRÄGTEM DRUCKGRADIENTEN

**Zusammenfassung**—Es wird über Messungen der mittleren Geschwindigkeit und Konzentration beim Einspritzen von Kohlendioxid durch eine gelochte Platte in eine Strömung berichtet. Die Bohrung bilden einen Winkel von 45° zur Plattenoberfläche und zum vorbeiströmenden Fluid. Es zeigte sich, daß bei mäßigem Druckgradienten in der Strömung die eingespritzte Flüssigkeit in turbulente Strömung übergeht und dadurch an der Plattenoberfläche wesentlich höhere Konzentrationen auftreten. Ein Turbulenzgrad von ungefähr 4% verringert bei ausgeprägtem Druckgradienten die Konzentrationen an der Wand um durchschnittlich 10%. Bei gleichförmiger Geschwindigkeit der Strömung ist dieser Effekt vernachlässigbar gering.

## ПЕРЕНОС ТЕПЛА К ПОДВИЖНОМУ ЗЕРНИСТОМУ СЛОЮ

**Аннотация** — Исследуется конвективный перенос тепла от плоской пластины, погруженной в подвижный зернистый слой. Разработана приближенная аналитическая модель, учитывающая частичечную структуру среды, и проведены измерения. Результаты показывают, что для данной конфигурации поверхности неоднородность среды при определенных условиях существенно влияет на число Нуссельта. Приводится полуэмпирическая корреляция, основанная на экспериментальных результатах для четырех различных типов гранулированных материалов.